Geographic and taxonomic patterns in aerobic traits of marine ectotherms

Justin L. Penn[1], Curtis Deutsch[1,2]

[1]Department of Geosciences and [2] High Meadows Environmental Institute, Princeton University, Princeton 08544, NJ, USA
*Correspondence and requests for materials should be addressed to jpenn@princeton.edu and cdeutsch@princeton.edu

Supplementary methods

Metabolic Index

The aerobic energy balance of an organism depends on temperature-dependent rates of O_2 supply (S) and metabolic demand (D), whose ratio can be represented by the Metabolic Index (Φ) as a function of ocean temperature (T) and oxygen partial pressure (pO_2) [1,2] (Table S1):

$$\Phi = \frac{S}{D} = A_o pO_2 \left(\frac{B}{B_{ref}}\right)^{\varepsilon} \exp\left\{\frac{E_o}{k_B}\left[\frac{1}{T} - \frac{1}{T_{ref}}\right]\right\} \quad \text{Eq. S1}$$

where A_o (atm^{-1}) is the species resting hypoxia tolerance, which is defined by the ratio of organismal O_2 supply rate (α_S, μmol O_2 $g^{-3/4}$ h^{-1} atm^{-1}) per unit pO_2 (atm) to resting metabolic O_2 demand rate (α_D, μmol O_2 $g^{-3/4}$ h^{-1}), both at a reference temperature (T_{ref}, K) and body size (B_{ref}, g):

$$A_o = \frac{\alpha_S}{\alpha_D} \quad \text{Eq. S2}$$

Variations in hypoxia tolerance due to body size (B) gradients are small relative to temperature because the allometric exponent of hypoxia tolerance (ε) is close to zero (i.e., $\varepsilon \approx 0$)[3].

The temperature dependence of resting metabolic rates and O_2 supply rates can be described by the exponential Arrhenius function of temperature (T) with activation energy E (in electron volts, eV): $Ar(E,T) = \exp\left\{\frac{-E}{k_B}\left[\frac{1}{T} - \frac{1}{T_{ref}}\right]\right\}$, which represents the thermal sensitivity of the rate of any process, or the ratio of such rates. Both resting metabolic rate and O_2 supply each have their own temperature sensitivities, E_d and E_s, respectively, the latter of which can reflect multiple steps in the organismal O_2 supply chain with distinct E_s, including diffusive O_2 flux across the water–body boundary, which is well-fit by an Arrhenius function, and ventilation and circulation rates, which are under biological control [4].

For resting hypoxia tolerance, its temperature sensitivity (E_o) is the difference between the effective activation energies for resting metabolic demand (E_d) and O_2 supply (E_s):

$$E_o = E_d - E_s \quad \text{Eq. S3}$$

The temperature dependence of resting hypoxia tolerance is often well described by the Arrhenius exponential function. For some species, divergence from simple exponential behavior can arise,

with hypoxia tolerance "flattening out" in cool water or even reversing in slope versus T, leading to thermal optima [4–6]. In dynamical models that directly simulate the time-dependent metabolism and O_2 supply of aquatic organisms, divergence from exponential behavior can be reproduced under a multi-step organismal O_2 supply if supply pathways have distinct temperature sensitivities (Fig. 1D) [4]. For example, thermal optima occur if O_2 supply is limited by a process that is more temperature-sensitive than metabolism at cold temperatures, such as external gill ventilation and/or internal blood circulation, and less sensitive at warm temperatures, like diffusion. The temperature-sensitivity of multi-step O_2 supply can be approximated by including a linear-temperature dependence of E_o (dE/dT), such that E_o itself varies with temperature [1], and causes reduced hypoxia tolerance at both warm and cool temperatures:

$$E_o(T) = E_o(T_{ref}) + \frac{dE}{dT}(T - T_{ref}) \quad \text{Eq. S4}$$

where $E_o(T_{ref})$ is the temperature-sensitivity at the T_{ref} (here in ^oC) and dE/dT is its linear temperature-dependence (eV/^oC), which can also be estimated from species state-space T-pO_2 (see below).

In nature, where metabolic rates are elevated by activity above the resting state, that resting rate (α_D) would be multiplied by the ratio of sustained active to resting metabolic rates, denoted Φ_{crit}, such that the ecological hypoxia tolerance (A_{eco}, atm^{-1}) is reduced by the same factor relative to that at rest:

$$A_{eco} = \frac{A_o}{\Phi_{crit}} \quad \text{Eq. S5}$$

In principle, Φ_{crit} may also vary with temperature. We assume that this ratio follows an Arrhenius function of temperature, with a distinct temperature sensitivity for Φ_{crit}, termed $E_{\Phi crit}$:

$$\Phi_{crit}(T) = \Phi_{crit} Ar(E_{\Phi_{crit}}, T) \quad \text{Eq. S6}$$

In Eq. S6, Φ_{crit} becomes the ratio of active to resting hypoxia tolerance at the reference temperature.

For active hypoxia tolerance, the net temperature sensitivity (E_{eco}) includes this additional component of active energy demand:

$$E_{eco} = E_o + E_{\Phi_{crit}} \quad \text{Eq. S7}$$

The aerobic energy balance of an organism in the active state then becomes:

$$\Phi = A_{eco} pO_2 \left(\frac{B}{B_{ref}}\right)^{\varepsilon} \exp\left\{\frac{E_{eco}}{k_B}\left[\frac{1}{T} - \frac{1}{T_{ref}}\right]\right\} \quad \text{Eq. S8}$$

In the ocean, the minimum pO_2 level for sustaining active aerobic metabolism (pO_2^{act}) can solved for from the active organismal O_2 balance at unity ($\Phi = 1$):

$$pO_2^{act} = \frac{1}{A_{eco}}\left(\frac{B}{B_{ref}}\right)^{-\varepsilon} \exp\left\{\frac{-E_{eco}}{k_B}\left[\frac{1}{T} - \frac{1}{T_{ref}}\right]\right\} \quad \text{Eq. S9}$$

Observations of lower pO_2 levels inhabited by a species as a function of water temperature in the environment can be fit to Eq. S9 to diagnose species active Metabolic Index traits (A_{eco}, E_{eco}). Active hypoxia tolerance (A_{eco}) measures the lower pO_2 that could be occupied by a species at T_{ref} and its temperature sensitivity (E_{eco}) measures how pO_2^{act} varies with T, with contributions from resting hypoxia tolerance (E_o) and the ratio of active to resting metabolic rates ($E_{\Phi crit}$). The traits needed to define the Metabolic Index for a given species in the resting state (A_o and E_o) can be calibrated from respirometry measurements of critical O_2 thresholds (pO_2^{crit}) versus temperature, which define the condition wherein the O_2 supply and resting metabolic demand are balanced ($\Phi = 1$) [1,2]. Within a species, the difference between diagnosed E_{eco} and measured E_o provides an estimate of how the ratio of sustained rates of activity to resting costs vary with temperature.

Biogeographic Data

To estimate the global distributions of species temperature-dependent hypoxia traits from biogeographic data, we downloaded 20,441,987 geospatial occurrences from the Ocean Biodiversity Information System (OBIS; https://obis.org/) for 25, 231 species with more than 10 unique occurrences when paired to hydrographic data from monthly climatological temperature and O_2 fields from the World Ocean Atlas (WOA) [7–9]. OBIS occurrences were downloaded in June of 2022. Species were restricted to 13 animal phyla (Arthropoda, Brachiopoda, Bryozoa, Chaetognatha, Chordata, Cnidaria, Ctenophora, Echinodermata, Hemichordata, Mollusca, Nematoda, Porifera, and Rotifera), which include 51 classes (Table S2). Occurrences were paired to hydrographic data by binning to the WOA grid at a resolution of 1° latitude and longitude and at 33 depths, from 0 m to 5500 m. Hydrographic conditions were determined at the central depth of the minimum and maximum depths reported by OBIS, or from either depth alone if only one metric was provided. Occurrences were discarded if the range of conditions within that depth range differed from the central estimate by more than 2 °C for temperature or 20% for O_2. For occurrences that did not have depth information altogether, we assigned a minimum depth at the sea surface and maximum depth at the seafloor. In cases in which even this maximum uncertainty in depths satisfied the error tolerance, the location data were retained. Non-animal marine groups and air-breathers (mammals, birds, reptiles, insects, arachnids, and centipedes) were excluded, leading to 25,090 species for further analysis. Species paired occurrences and hydrographic conditions were binned onto a grid of temperature and pO_2 (state-space T-pO2) for diagnosis of species traits and to a 5° latitude-longitude grid for mapping.

Trait Estimation Procedure

We estimated species traits by evaluating the minimum pO_2 level as a function of temperature that best defines their observed T-pO_2 occurrence range boundary. Traits were diagnosed as the values that maximizes the predictive skill of Φ (Eq. S9) in segregating inhabited and uninhabited grid cells, using a standard statistical categorization metric, the F1-score [10]. The F1-score is computed based on the presence and absence of a species on a regular grid of T and pO_2, for which the environmental conditions fall above a lower threshold pO_2 value (pO_2^{act}; Eq. S9) and was used to find the optimal combination of species traits (A_{eco}, E_{eco}, and dE/dT).

The F1-score is calculated as the harmonic mean of precision and recall, with equal weighting given to both measures [1,10]. Precision measures the probability that the presence of the species in waters for which $pO_2 \geq pO_2^{act}$ is a true positive (TP; specimen reported in the space in which they are predicted to occur) rather than a false positive (FP; specimen reported in a space predicted to be below the pO_2 threshold). Recall is the probability that a specimen is actually reported where $pO_2 > pO_2^{act}$ (that is, how likely is a true positive relative to a false negative (FN); missing observations above pO_2^{act}). In terms of these variables, the F1-score can be expressed as:

$$F_1 = \left(\frac{recall^{-1}+precision^{-1}}{2}\right)^{-1} = \frac{2TP}{2TP+FN+FP} \quad \text{Eq. S10}$$

This metric does not give weight to true absence data (species not found in a location), which is inconsistently reported in OBIS data. A model with perfect precision and recall would have F1 = 1 (no false negatives or positives). Diagnosed traits were those that yielded the global maximum F1-score. Species with low F1 scores were discarded from further analysis (F1 < 0.5) but the filtering threshold has little impact on the distributions of E_{eco} and A_{eco} (Fig. S1). In general, F1-scores increased with the number of occurrence observations per species, indicating that low score were likely the result of poor sampling as opposed to poor model skill.

For each species, we evaluated the model fit both while allowing for a temperature-dependent E_{eco} ($dE/dT > 0$) and for the case where E_{eco} is constant ($dE/dT = 0$), discarding the model fit and traits with the lower F1-score. In the case of constant E_{eco}, traits were fit to lower pO_2 thresholds at the warm edge of a species temperature range, that is, for T above the median T. For species with $dE/dT > 0$, analyses of E_{eco} were computed at the species median inhabited T, i.e., $E_{eco}(T_{med})$.

In total, the filtering and fitting procedures yield trait estimates for 24,852 out of the 25,090 species. Traits could not be robustly derived for the remaining 238 species (<1% of species that meet the filtering criteria) because the fitting algorithm did not converge on a solution to Eq. S9. These species were included in the .mat file in the supplementary material but are assigned NaN values for traits and are not included in the analysis.

In the diagnosis of $E_{\Phi crit}$, we estimated this trait as the difference between diagnosed E_{eco} from OBIS and measured E_o from laboratory experiments (Eq. S7) for all species with both traits available. For this species-specific analysis, the E_{eco} of each species was diagnosed over the same temperature range as their experimental E_o and used a constant E_{eco} (i.e., $dE/dT = 0$). This was done for consistency with the method for deriving laboratory E_o and because the Arrhenius function captures much of the thermal variation in resting hypoxia tolerance over the limited temperature range of respirometry experiments.

Phylogenetic Tree of life.

Phylogenetic relationships among species were established using the Open Tree of Life (OTL, https://tree.opentreeoflife.org)[11], following the methods of [12]. Species names were looked up in the OTL, and only those with precise matches were retained. Species with OBIS traits not found in the OTL were excluded, as were those with information in the OTL but not OBIS. For ease of visualization and to reduce computational costs, phylogenetic analyses were limited to a subset of species with the best fits and highest quality of state-space T-pO_2 data, i.e., F1-scores ≥ 0.8 and median depths greater than 10 m, chosen because of the potential for high amplitude pO_2 variability

at the surface, which is poorly resolved in climatological observations [13]. This leads to 1,997 tree tips (species) and 1,446 internal nodes. Branch lengths were set equal to the number of descendant tips minus one, following the method of [14]. We use a Grafen's rho scaling parameter equal to 0.4, which was found to best explain observed variations in resting hypoxia tolerance in fishes [12], and expands the branch lengths near the tree tips relative to the tree root. We tested for a phylogenetic signal in traits in a larger group of species (F1-score > 0.5 and median depth > 10 m) (13,170 tree tips and 6,200 internal nodes) using the function 'phylosig' in R, and found that both E_o and $\log_{10}(A_c)$ show a significant phylogenetic signal (Pagel's lambda , $\lambda = 0.54$ (0.47-0.86) and 0.74 (0.7-0.95), respectively, and $p << 0.001$) across a wide range of Grafen's rho parameter ($\rho = 0.4$ central value, 0.2-1 range), consistent with directly measured resting hypoxia tolerance in a group of nearly 200 fishes [12].

Laboratory estimates of $E_{\Phi crit}$

We estimated the temperature dependence of the ratio of active to resting metabolic rates ($E_{\Phi crit}$) using laboratory measurements of the ratio of maximum metabolic rates (MMR) to resting metabolic rates (RMR), termed factorial aerobic scope (FAS), at multiple temperatures, as a proxy for Φ_{crit}. We compiled FAS data from published studies of five marine species (n = 6 experiments) that have estimates of active and resting hypoxia traits in our database, including four fish and one scallop [15–18]. E_{crit} was determined from linear regression of log FAS versus temperature, substituting FAS for $\Phi_{crit}(T)$ in Eqn S6. This comparison is necessarily approximate because sustained activity in nature lies between resting and maximum metabolic rates and would include biological processes not resolved in short term MMR experiments, such as reproduction, feeding and growth, in addition to uncertainty in laboratory measurements. Nevertheless, it serves as a useful initial check on the expectation of a lower temperature-dependence of active hypoxia tolerance (E_{eco}) compared to the resting state (E_o), as predicted by the analysis of OBIS data.

References

1. Deutsch C, Penn JL, Seibel B. 2020 Metabolic trait diversity shapes marine biogeography. *Nature* **585**, 557–562. (doi:10.1038/s41586-020-2721-y)

2. Deutsch C, Ferrel A, Seibel B, Pörtner H-O, Huey RB. 2015 Climate change tightens a metabolic constraint on marine habitats. *Science* **348**, 1132–1135. (doi:10.1126/science.aaa1605)

3. Deutsch C, Penn JL, Verberk WCEP, Inomura K, Endress M-GA, Payne JL. 2022 Impact of warming on aquatic body sizes explained by metabolic scaling from microbes to macrofauna. *PNAS* **119**, 9. https://doi.org/10.1073/pnas.2201345119

4. Endress M-GA, Boag TH, Burford BP, Penn JL, Sperling EA, Deutsch CA. 2022 Physiological causes and biogeographic consequences of thermal optima in the hypoxia tolerance of marine ectotherms. bioRxiv (doi:10.1101/2022.02.03.478967)

5. Boag TH, Stockey RG, Elder LE, Hull PM, Sperling EA. 2018 Oxygen, temperature and the deep-marine stenothermal cradle of Ediacaran evolution. *Proc. R. Soc. B.* **285**, 20181724. (doi:10.1098/rspb.2018.1724)

6. Duncan MI, James NC, Potts WM, Bates AE. 2020 Different drivers, common mechanism; the distribution of a reef fish is restricted by local-scale oxygen and temperature constraints on aerobic metabolism. *Conservation Physiology* **8**, coaa090. (doi:10.1093/conphys/coaa090)

7. Locarnini, R. A., A. V. Mishonov, O. K. Baranova, T. P. Boyer, M. M. Zweng, H. E. García, J. R. Reagan, D. Seidov, K. Weathers, C. R. Paver, and I. Smolyar,. 2019 World Ocean Atlas 2018, Volume 1: Temperature. A. Mishonov Technical Ed. *NOAA Atlas NESDIS* 81, 52pp.

8. Garcia H, et al. 2018 K. Weathers, C. R. Paver, I. Smolyar, T. P. Boyer, R. A. Locarnini, M. M. Zweng, A. V. Mishonov, O. K. Baranova, D. Seidov, and J. R. Reagan, 2019. World Ocean Atlas 2018, Volume 3: Dissolved Oxygen, Apparent Oxygen Utilization, and Oxygen Saturation. A. Mishonov Technical Ed.; NOAA Atlas NESDIS 83, 38pp.

9. OBIS. 2022 Ocean Biodiversity Information System. Intergovernmental Oceanographic Commission of UNESCO. See www.obis.org.

10. Howard EM *et al.* 2020 Climate-driven aerobic habitat loss in the California Current System. *Sci. Adv.* **6**, eaay3188. (doi:10.1126/sciadv.aay3188)

11. OpenTree et al.,. 2023 Open Tree of Life Synthetic Tree. (doi:https://doi.org/10.5281/zenodo.3937741)

12. Verberk WCEP, Sandker JF, van de Pol ILE, Urbina MA, Wilson RW, McKenzie DJ, Leiva FP. 2022 Body mass and cell size shape the tolerance of fishes to low oxygen in a temperature-dependent manner. *Global Change Biology* **28**, 5695–5707. (doi:10.1111/gcb.16319)

13. Lucey NM, Deutsch CA, Carignan M-H, Vermandele F, Collins M, Johnson MD, Collin R, Calosi P. 2023 Climate warming erodes tropical reef habitat through frequency and intensity of episodic hypoxia. *PLOS Clim* **2**, e0000095. (doi:10.1371/journal.pclm.0000095)

14. Grafen A. 1989 The phylogenetic regression. *Philosophical Transactions of the Royal Society B: Biological Sciences* **326**, 119–157.

15. Slesinger E, Andres A, Young R, Seibel B, Saba V, Phelan B, Rosendale J, Wieczorek D, Saba G. 2019 The effect of ocean warming on black sea bass (Centropristis striata) aerobic scope and hypoxia tolerance. *PLoS ONE* **14**, e0218390. (doi:10.1371/journal.pone.0218390)

16. Ern R, Norin T, Gamperl AK, Esbaugh AJ. 2016 Oxygen-dependence of upper thermal limits in fishes. *Journal of Experimental Biology*, **219**, jeb.143495. (doi:10.1242/jeb.143495)

17. Ern R, Johansen JL, Rummer JL, Esbaugh AJ. 2017 Effects of hypoxia and ocean acidification on the upper thermal niche boundaries of coral reef fishes. *Biol. Lett.* **13**, 20170135. (doi:10.1098/rsbl.2017.0135)

18. Schalkhausser B, Bock C, Pörtner H-O, Lannig G. 2014 Escape performance of temperate king scallop, Pecten maximus under ocean warming and acidification. *Mar Biol* **161**, 2819–2829. (doi:10.1007/s00227-014-2548-x)

259 Table S1. Definitions of mathematical symbols

A_{eco}	Species active hypoxia tolerance (atm^{-1}), equivalent to the resting hypoxia tolerance divided by the ratio of active to resting metabolic rates, $A_{eco} = A_o/\Phi_{crit}$ and diagnosed from OBIS occurrences paired with T-pO_2.
A_o	Species resting hypoxia tolerance (atm^{-1}) or the ratio of O_2 supply (α_S) to demand (α_D), measurable as $1/pO_2^{crit}$ at the reference temperature (T_{ref}).
Φ_{crit}	Species-specific minimum Φ threshold (unitless) required to support a long-term population in the environment, corresponding to the ratio of sustained rates of activity to resting metabolism, and which can depend on temperature.
$Ar(E,T)$	The Arrhenius exponential factor (unitless) describes how biological rates and pO_2^{crit} vary with temperature, where E is the temperature sensitivity (electronvolts, eV), k_B is Boltzmann's constant (eV/K), and T_{ref} is the reference temperature (K).
E_{eco}	The temperature sensitivity of active hypoxia tolerance (eV), equal to the sum resting tolerance (E_o) and the ratio of active to resting costs ($E_{\Phi crit}$) and diagnosed from OBIS occurrences paired with T-pO_2.
E_o	The temperature sensitivity of resting hypoxia tolerance (eV), equal to the difference between the temperature sensitivity of resting metabolic demand (E_d) and O_2 supply (E_s), and measurable from the slope of $\ln(pO_2^{crit})$ versus $1/k_BT$.
$E_{\Phi crit}$	The temperature sensitivity (eV) of the ratio of sustained active to resting rates of metabolism, Φ_{crit}, equal to the difference between the temperature sensitivity of active and resting hypoxia tolerance: $E_{\Phi crit} = E_{eco} - E_o$
E_d	The temperature sensitivity of resting metabolic rate (eV).
E_s	The temperature sensitivity of O_2 supply (eV), calculated from $E_s = E_d - E_o$.
dE/dT	The linear-temperature dependence of E_{eco} or E_o (units of eV/^oC), which captures the temperature-sensitivity of a multi-step O_2 supply.
α_D	The metabolic rate (mol O_2 per unit of body mass per time) at reference temperature and body size.
α_S	The O_2 supply coefficient (mol O_2 per unit of body mass per time per atm) at reference temperature and body size, calculated from $\alpha_S = Ao*\alpha_D$.
FAS	Factorial aerobic scope, equal to the ratio of maximum metabolic rates (MMR) to resting metabolic rates (RMR) measured in laboratory experiments
pO_2	Oxygen partial pressure (atm)
T	Temperature (K unless otherwise specified)
V_h	Species resting hypoxia vulnerability at the reference T, equivalent to $1/A_o$, or the ratio of resting O_2 demand (α_D) to supply (α_S) and measurable as pO_2^{crit} at the reference temperature (T_{ref}).

260
261

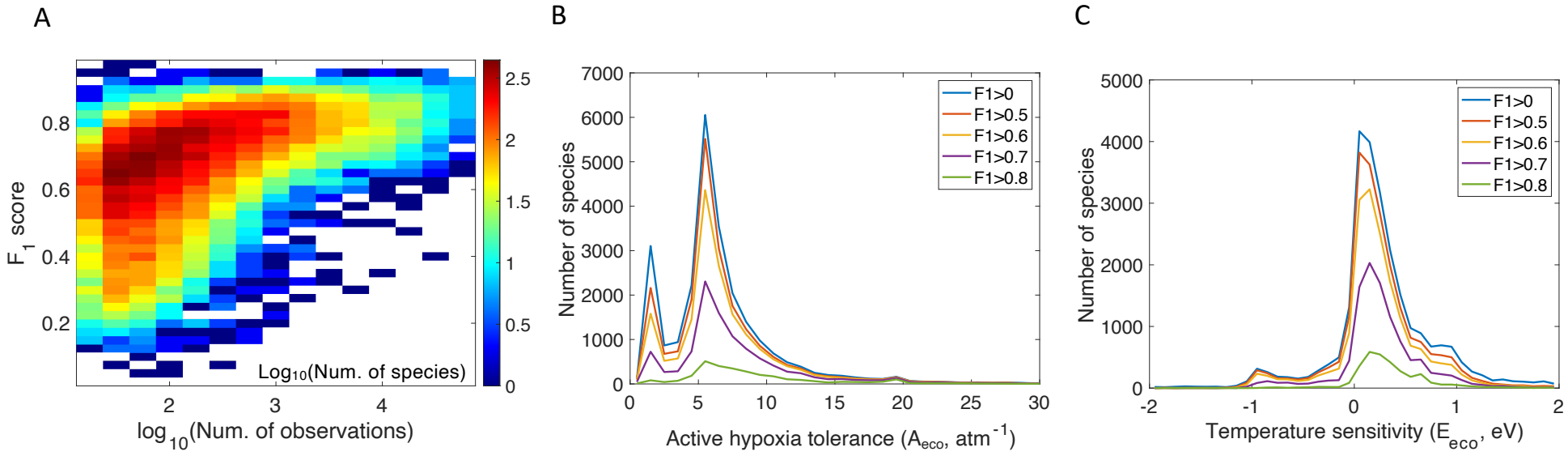

Figure S1. Statistics of fits for diagnosed species traits. (A) Bivariate histogram showing the fit (F1-score) of species diagnosed pO_2^{act} versus the number of occurrence observations per species. (B, C) The distributions of A_{eco} and E_{eco} are largely insensitive to the minimum F1-score threshold used to filter species.

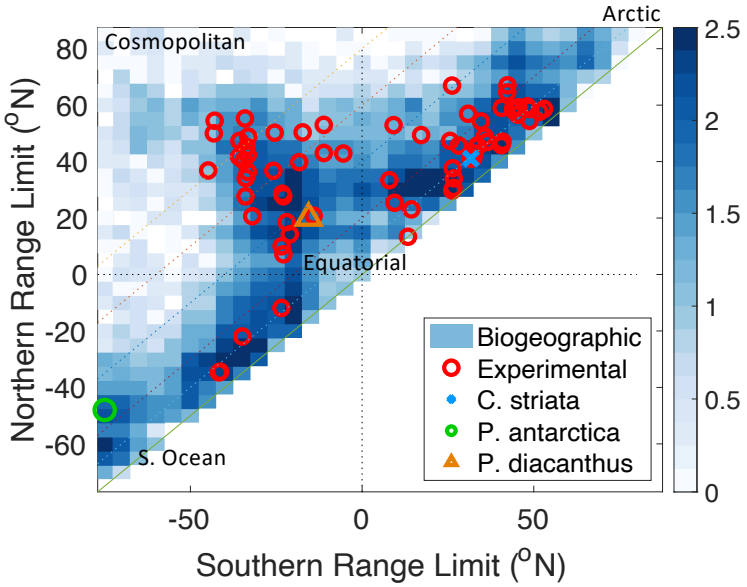

Figure S2. Range limits of species with trait estimates. Species with direct trait measurements (red points) are found in the most frequently sampled latitudes in the biogeographic data (blue shading). The trait database contains global coverage, including cosmopolitan species, and those endemic to the northern and southern hemisphere's polar and mid-latitude waters, and the tropics. Latitude ranges are based on 5th and 95th percentiles. Range limits of example species from Fig. 1 are shown.

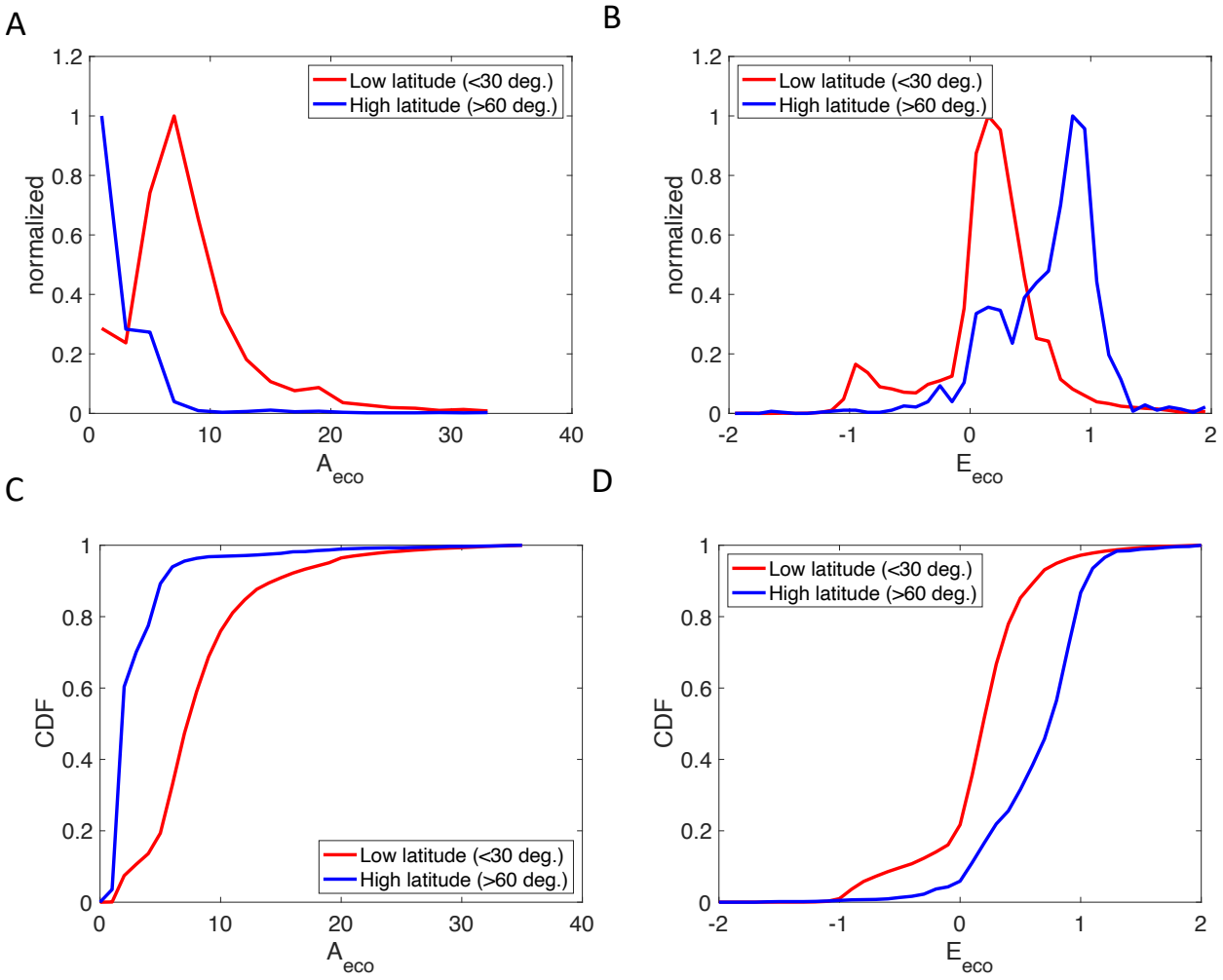

Figure S3. Histograms (A,B) and cumulative distribution functions (C,D) of species traits in the low (<30°) versus high latitudes (>60°). In the low latitudes, species display a higher active hypoxia tolerance (higher A_{eco}) that decreases less with temperature (lower E_{eco}) compared to high latitudes. Distributions are normalized to the maximum number of species in each region.

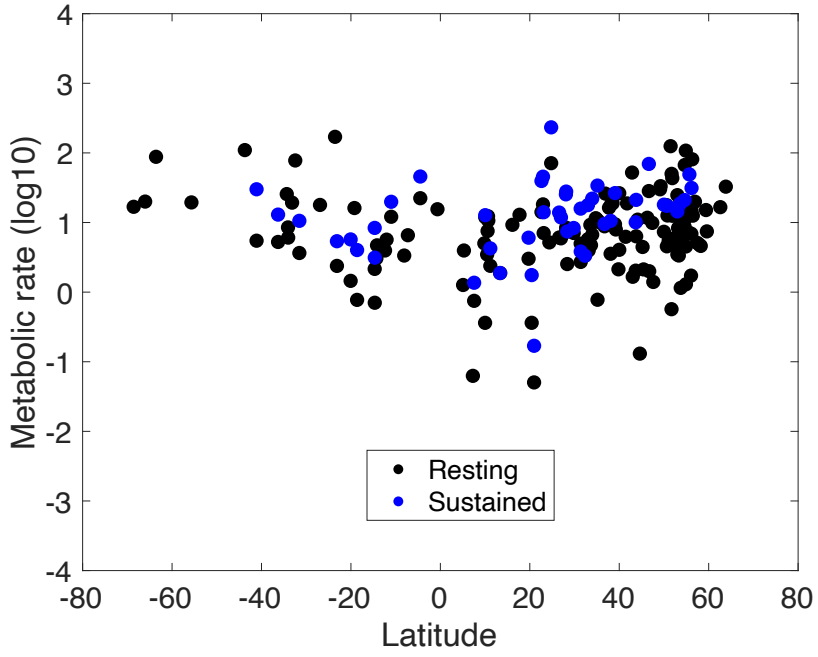

Fig. S4. Latitudinal gradients in species metabolic traits from experimental measurements [1]. Temperature-normalized metabolic rates of O_2 demand in a state of rest (α_D; black circles) and sustained activity (blue circles) decline slightly in lower latitudes. Active (sustained) metabolic rates are the product of resting metabolic rate (α_D) and the average ratio of sustained to resting metabolic rate ($\mathbf{\Phi}_{crit}$). Traits are plotted at species median latitudes from occurrence data.

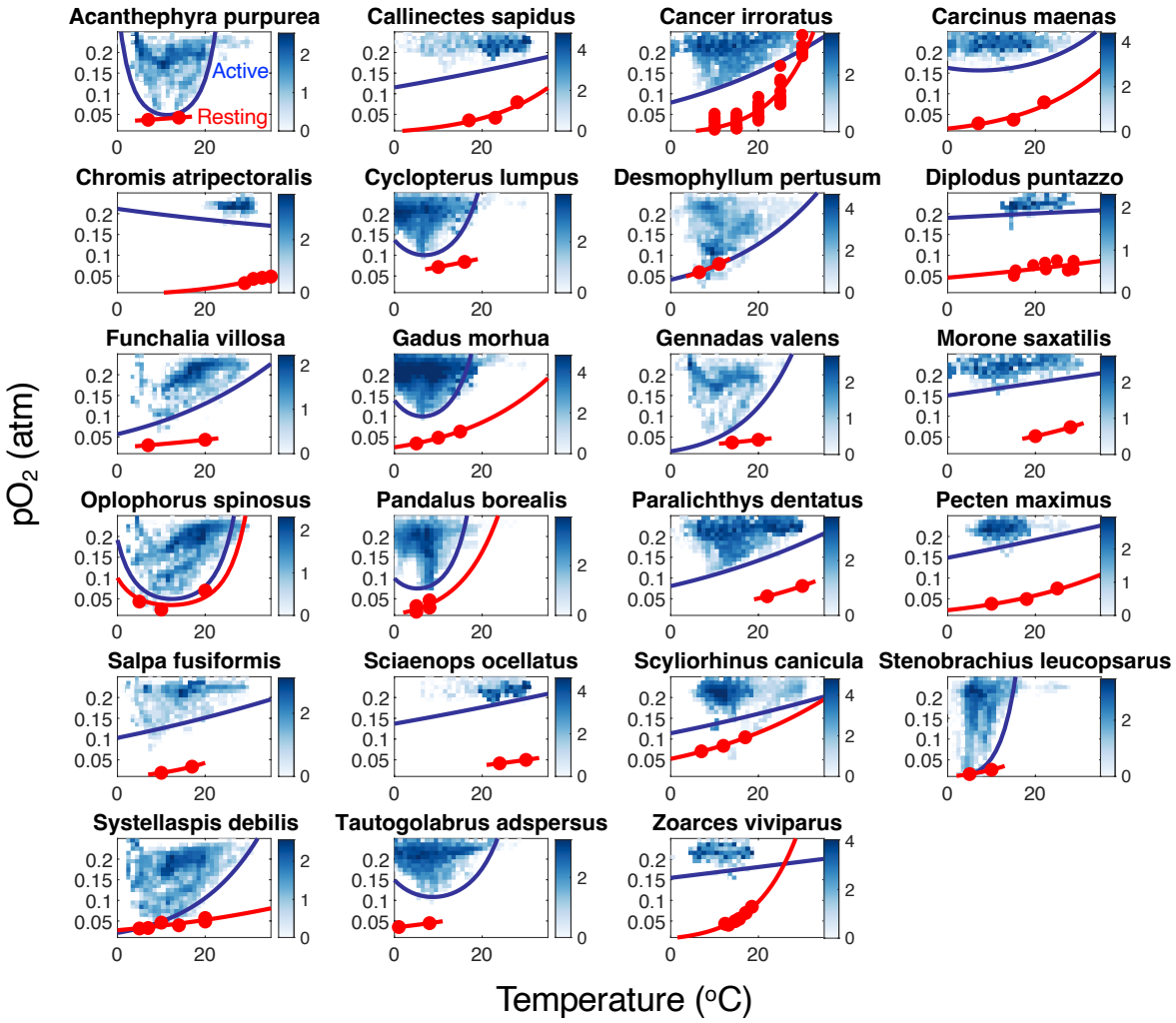

Figure S5. Temperature-dependent hypoxia thresholds estimated from biogeographic data and laboratory experiments. Species occurrences in T-pO_2 state-space (blue shading) reveal how the minimum pO_2 inhabited by a species in the ocean (pO_2^{act}) varies with T. This active T-dependence (E_{eco}) reflects the T-dependence of resting hypoxia tolerance (E_o) measured by pO_2^{crit} (red points) and the T-dependence of the ratio of active to resting metabolic costs ($E_{\Phi crit}$). Hypoxia tolerance (A_o, resting and A_{eco}, active) and its temperature sensitivity (E_o and E_{eco}) are estimated by fitting a model of the ratio of O_2 supply to demand (Eq. S1,8; lines) to experimental pO_2^{crit} data (red) and inhabited lower pO_2 levels as a function of T based on the paired climate-occurrence data (blue). Resting hypoxia thresholds are extrapolated across the full T range for species with more than two pO_2^{crit} measurements. Plots are shown for species with F1>0.77. Color fields are number of species occurrences (log_{10}). pO_2^{crit} data are from [1].

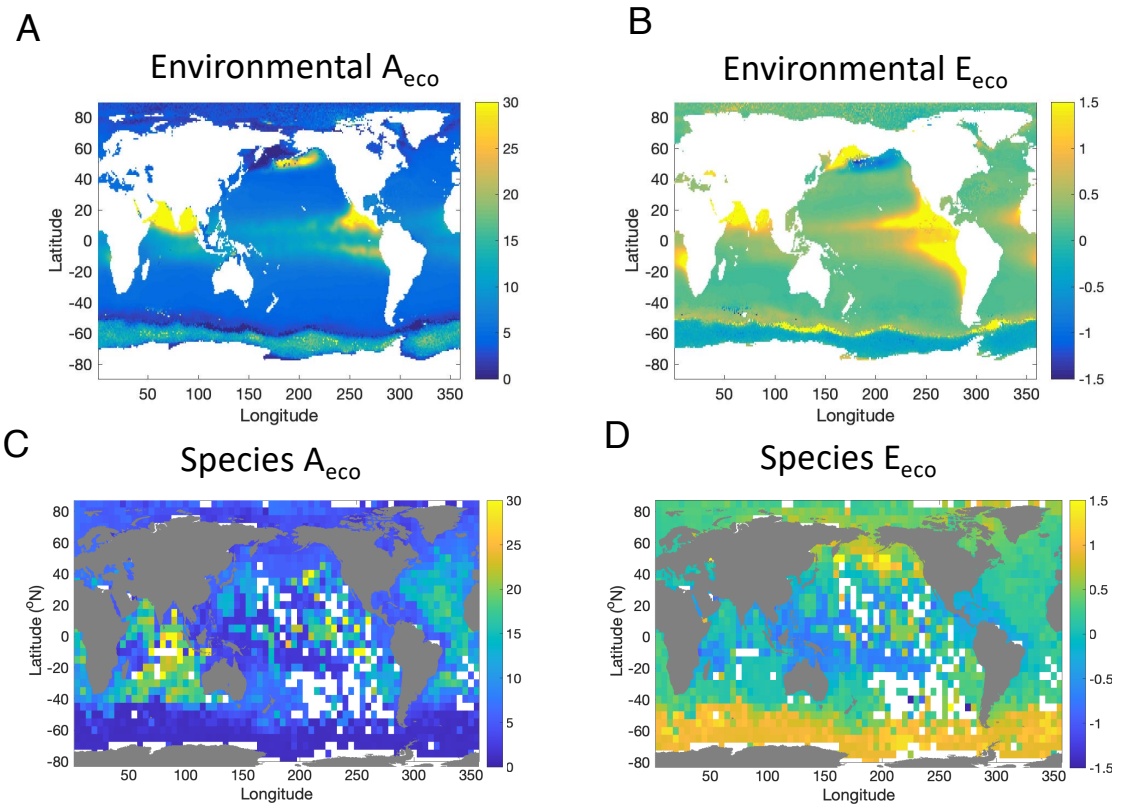

Fig. S6. Spatial patterns of species A_{eco} and E_{eco} are not driven by local environmental gradients. (A,B) Patterns of environmental A_{eco} and E_{eco} are diagnosed from local variability of T-pO_2 state space over time (monthly) and depth (0-500m) for each vertical profile across all latitude and longitudes (i.e., without using species occurrence data). Major features in environmental traits are not found in species A_{eco} and E_{eco} (C, D), as would be expected if diagnosed species traits were an artifact of the ocean's vertical stratification or of poorly sampled geographic ranges. These environmental features include large, contiguous spikes in A_{eco} and E_{eco} around tropical suboxic zones and strong gradients across the N. Pacific, which are not present in species traits. In addition, the strong gradient across the southern polar frontal zone is of the opposite sign compared to the gradient in species traits. Environmental and species traits are fit using dE/dT and E_{eco} is plotted at the median T.

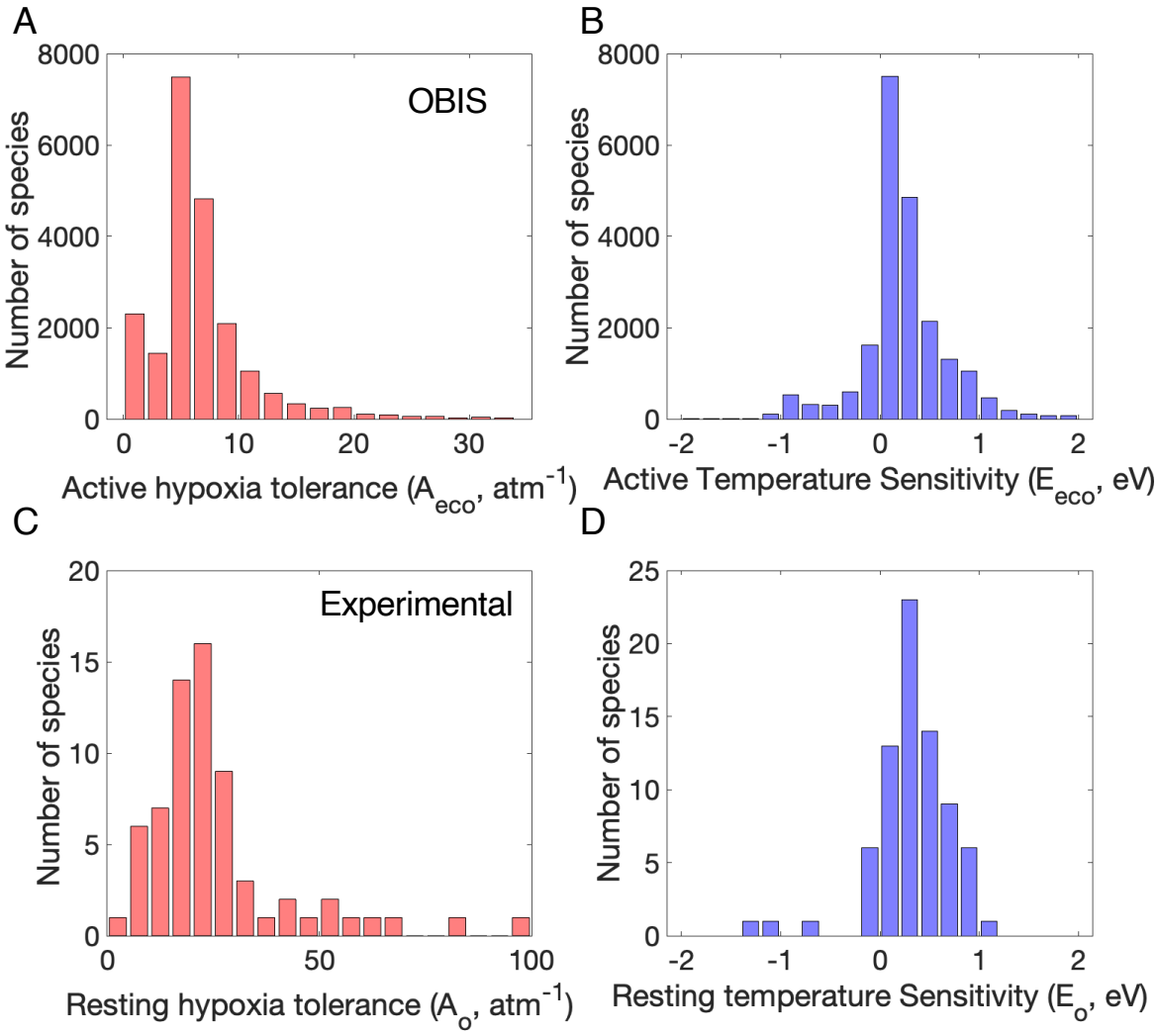

Figure S7. Distributions of active hypoxia thresholds (A_{eco}) and temperature sensitivities (E_{eco}) are diagnosed from biogeographic occurrence data (A,B). Resting traits (A_o and E_o) are estimated from direct respirometry experiments of pO_2^{crit} vs. T (C,D).